Dielectric anomalies in bismuth-doped $SrTiO_3$: Defect modes at low impurity concentrations

Chen Ang,* Zhi Yu,* J. Hemberger, P. Lunkenheimer, and A. Loidl
Institut für Physik, Universität Augsburg, D-86135 Augsburg, Germany
(Received 8 September 1998)

The dielectric relaxation modes in low bismuth doped $SrTiO_3$ were studied at temperatures 1.5–300 K and frequencies up to 1.8 GHz. We observe two modes, at 8 K (mode I) and 65 K (mode V), which also occur in single-crystalline $SrTiO_3$. With Bi doping, two further dielectric peaks, 18 K (mode II) and 30 K (mode III), are induced in both real and imaginary parts of the permittivity on the quantum paraelectric background; the large paraelectric permittivity of pure $SrTiO_3$ is strongly reduced. This fact signals the suppression of quantum fluctuations and concomitantly the appearance of polar clusters. The dynamics of these modes is studied and the physical nature is discussed. Mode I, which has been previously explained in terms of the coherent quantum state, is possibly due to an unknown defect mode. Mode V seems to be induced by the ferroelastic domain-wall dynamics. We attribute mode III to the existence of the noninteracting polar clusters, which may be coupled with some intrinsic mechanism of the host lattice. Mode II is tentatively explained in terms of polaronic relaxation. [S0163-1829(99)03506-7]

I. INTRODUCTION

At low temperatures $SrTiO_3$ (STO) and $KTaO_3$ (KTO) reveal a highly enhanced but temperature-independent permittivity. It is thought that both systems are on the verge of ferroelectricity, but the quantum fluctuations stabilize the paraelectric phase.[1,2] However, when doped with moderate amounts of impurities,[3–7] or in external electric fields,[8] polar order is induced, the character of which depends on the particular system and on the defect concentration. The low-temperature phases in the doped compounds have been interpreted rather controversially: as model systems of dipolar glasses,[6] as long-range, and as short-range-ordered polar states.[9–11]

After an earlier study by Mitsui and Westphal,[12] Bednorz and Müller[4] reported the occurrence of an *XY* quantum ferroelectric state at low Ca doping, and a crossover to a diffusive ferroelectric state with increasing Ca concentration. The relaxation dynamics of the polar distortions around the impurity site in Ca-doped STO near the quantum limit was studied by Kleemann *et al.*[13] in detail. They found an enhanced dielectric loss on the low-frequency tail of the dielectric loss peaks and attributed it to dynamic heterogeneities due to the thermally activated relaxation of dynamically coupled mesoscopic domains.[13] These results were explained within the model of dynamically correlated domains.[14]

In this paper we continue our systematic studies of STO doped with trivalent defects (e.g., Bi, La, etc.), which displays some different behavior from the divalent Ca doping.[15–17] In the present paper we extend the frequency and the temperature range up to 1.8 GHz and down to 1.5 K, respectively, and the lowest Bi doping is extended to 0.05 at %. We focus especially on the very low Bi concentration regime. We report on the occurrence of five distinct relaxation modes showing up as peaks in the dielectric loss ε'', which in the real part ε' are superimposed on the paraelectric background of the host lattice of STO. We study the relaxation dynamics of these modes and try to explain their physical origin. In the present paper the results for low Bi concentrations are shown. In the following paper[18] we present the results for $x \geqslant 0.0033$ with special emphasis on the relaxor ferroelectric properties arising at high concentrations.

II. EXPERIMENTAL DETAILS

The ceramic samples of $(Sr_{1-1.5x}Bi_x)TiO_3$ with Bi content x in the range of $0 \leqslant x \leqslant 0.167$ were prepared by solid-state reaction. More details for sample preparation can be found in Ref. 15. X-ray-diffraction results at room temperature revealed that all the samples crystallize in the cubic phase. Energy-dispersion analyses indicate a homogeneous distribution of the Bi, which is, within experimental errors, in agreement with the nominal composition.

For measurements of the dielectric properties in the low-frequency region, $20\,\mathrm{Hz} \leqslant \nu \leqslant 1\,\mathrm{MHz}$, an autobalance bridge (HP4284 LCR meter) was used. For the measurements in the radio frequency range, $1\,\mathrm{MHz} \leqslant \nu \leqslant 1.8\,\mathrm{GHz}$, the sample was mounted at the end of a home-built coaxial air line, connecting the inner and outer conductors. The complex dielectric permittivity was recorded using an HP4291A impedance analyzer. In order to eliminate the influence of the coaxial line, a calibration using three standard samples was performed. For both methods the applied ac field was 1 V/mm. We checked that the dielectric permittivity is independent of the electrodes and of the sample's thickness. The temperature dependence of the dielectric properties was measured in a home-built cryostat for temperatures $1.5 \leqslant T \leqslant 300\,\mathrm{K}$. Cooling or heating rates of 0.4 K per minute were utilized.

III. RESULTS

A. Phase diagram

As reported in previous publications,[15,16] several dielectric loss peaks appear as Bi is incorporated into STO; all of them display frequency dispersion. In Fig. 1 we present the plot of $\varepsilon''(T)$ at 100 Hz for Bi concentrations $0 \leqslant x \leqslant 0.0033$. Five different relaxation modes can be identified. For nominally pure STO, only two peaks appear, close to 8 K at 100 Hz (mode I) and close to 65 K at 100 Hz (mode V). These relaxation modes also show up at low x and their

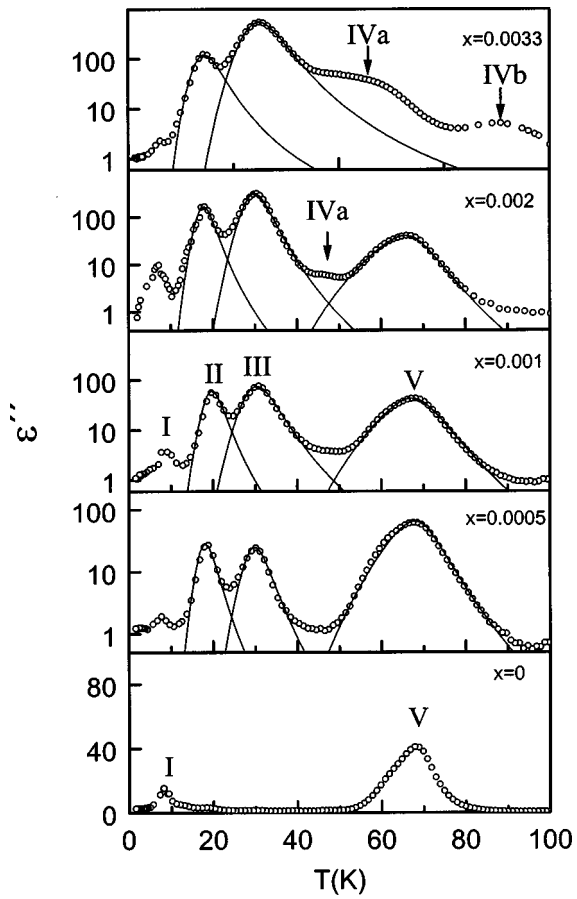

FIG. 1. Temperature dependence of the imaginary part of permittivity for $(Sr_{1-1.5x}Bi_x)TiO_3$ with $0 \leqslant x \leqslant 0.0033$ at 100 Hz. The lines were calculated assuming a Cole-Cole distribution of relaxation times and a thermally activated relaxation time.

strength only weakly depends on the impurity concentration. Similar polar modes have been observed previously in pure STO.[8,19,20] However, even for very low Bi doping, at ppm level ($x=0.0005$), two further peaks appear. These relaxation peaks indexed with II and III are well defined at low doping concentrations. In this concentration regime they dominate the relaxation spectra and can be observed close to 18 and 30 K at 100 Hz, respectively. The temperatires of peak maxima are almost independent of x while the intensity roughly scales with the bismuth concentration. Obviously these peaks represent impurity defect modes of polar and/or electronic origin. With increasing Bi concentration a new broad relaxation peak evolves (ferroelectric relaxor mode IV) that strongly depends on impurity concentration.[18]

Figure 2 shows a summary of the dielectric relaxation modes for concentrations $x \leqslant 0.167$ in the form of a phase diagram, which includes the high-concentration results reported in the following paper.[18] Modes I, II, and III vanish at high Bi concentrations. For $x \geqslant 0.0033$, mode V is no longer visible due to the occurrence of a new broad relaxation peak (IVa) which can be identified as relaxor mode.[18] A precursor of this mode may be already seen between peaks III and V for $x=0.002$ (Fig. 1). Another mode (IVb) arises for $x \geqslant 0.0033$ at a somewhat higher temperature (87 K at 100 Hz, Fig. 1) and seems to merge with mode IVa for $x \geqslant 0.04$ into the relaxor mode. Relaxor mode IV is the only one that survives for bismuth concentration $x \geqslant 0.1$.[18]

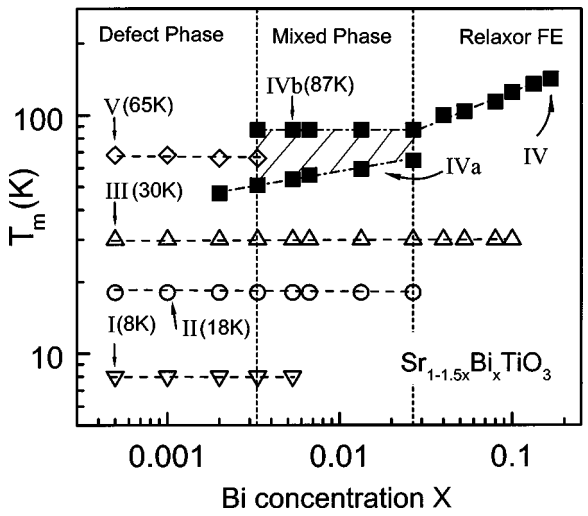

FIG. 2. Phase diagram of relaxation modes in $(Sr_{1-1.5x}Bi_x)TiO_3$ ($x=0.002-0.167$). T_m is the temperature of the dielectric loss peak at 100 Hz.

In this paper we will focus primarily on the relaxation dynamics of the relaxation modes II and III at low bismuth concentration. As a prototype example we show the results for STO doped with 0.2 at % bismuth. We also briefly comment on the relaxation modes I and V. Mode IV will be discussed in the following paper.[18]

B. Relaxation modes for $x=0.002$

Figure 3 shows the temperature dependence of the real (upper panel) and imaginary parts (lower panel) of the complex dielectric permittivity for Bi-doped STO ($x=0.002$) at different measuring frequencies. The relaxation modes II and III are clearly detectable in both real and imaginary part. These two processes appear in addition to the paraelectric

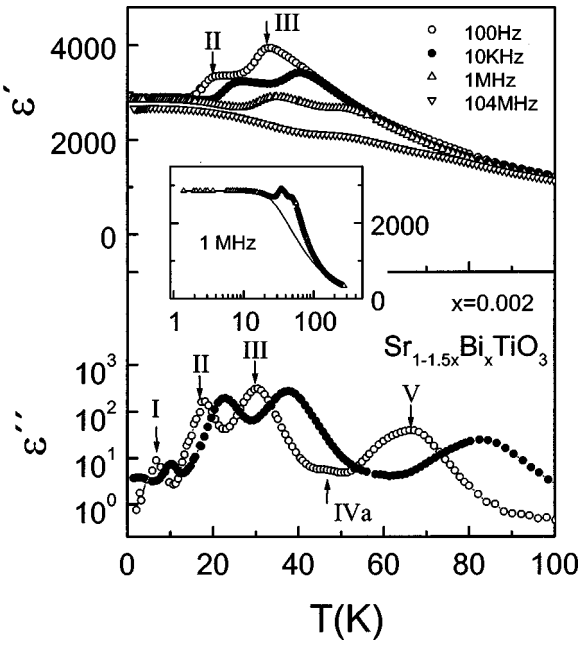

FIG. 3. Temperature dependence of ε' and ε'' for various frequencies in $(Sr_{1-1.5x}Bi_x)TiO_3$ ($x=0.002$). The inset shows $\varepsilon'(\nu)$ for 1 MHz with a fit to the Barrett relation, Eq. (1).

background of the host lattice of STO. However, the low-temperature dielectric constant is strongly reduced as a function of Bi concentration and roughly follows a relation $\varepsilon_{0\,\mathrm{K}} := \varepsilon'(T \to 0\,\mathrm{K}) \propto 1/x$, similar to the observation for Li-doped KTO by Höchli, Weibel, and Boatner.[5] This experimental fact possibly signals the existence of local order in the doped compounds, making the system less susceptible. However, substantial paraelectric regions survive down to the lowest temperatures even in the doped compounds.

The paraelectric background of pure and doped $SrTiO_3$ can be described by the Barrett relation[21] which is a mean-field theory taking quantum fluctuations into account:

$$\varepsilon' = C/[(T_1/2)\coth(T_1/2T) - T_0]. \quad (1)$$

C is the Curie-Weiss constant, T_1 is the quantum fluctuation starting temperature, and T_0 is the temperature where the lattice instability occurs. A fit of the Barrett relation to the experimental data neglecting the relaxation contributions is shown in the inset in Fig. 3. As best-fit parameters, we found $T_1 = 84\,\mathrm{K}$, $T_0 = 10.4\,\mathrm{K}$, and $C = 9 \times 10^4\,\mathrm{K}$ for $x = 0.002$. The parameters C and T_1 are similar to those reported for a pure single crystal by Müller and Burkard ($T_1 = 84\,\mathrm{K}$, $T_0 = 38\,\mathrm{K}$, and $C = 9 \times 10^4\,\mathrm{K}$).[1] However, T_0 is strongly reduced for the doped compound. As described by Barrett,[21] the larger ratio $T_1/2T_0$ implies that the system is much further away from the ferroelectric instability.

It is well known that the Lyddane-Sachs-Teller (LST) relation is valid for pure STO.[2] For $x = 0.002$, ε' is smaller roughly by a factor of ~ 4 as compared with that of pure STO. Assuming that the LST relation is also valid for Bi-doped STO, the soft-mode frequency at $T \to 0\,\mathrm{K}$ of the sample with $x = 0.002$ should be increased by a factor of 2. The test of the validity of the LST relation in Bi-doped $SrTiO_3$ will be an interesting subject for further investigations.

For a better understanding of the microscopic processes underlying the observed relaxation modes we performed a detailed analysis. Figure 4 shows the frequency dependence of ε'' for different temperatures for the relaxation modes II and III. The two-peak behavior can be clearly detected. Both relaxation processes were analyzed assuming a symmetric distribution of relaxation rates and utilizing the Cole-Cole type of function:

$$\varepsilon^* = \varepsilon_\infty + (\varepsilon_0 - \varepsilon_\infty)/[1 + (i\omega\tau)^{1-\alpha}]. \quad (2)$$

ε_0 is the static permittivity, ε_∞ is the high-frequency permittivity, ω is the angular frequency, τ is the mean relaxation time, and α is the width parameter leading to a symmetric broadening of the Debye relaxation. The Debye case is recovered for $\alpha = 0$ while $\alpha = 1$ indicates an infinitely broad distribution of relaxation times. The permittivity curves for all samples were fitted with a least-square approach, yielding the static susceptibility $\Delta\varepsilon (= \varepsilon_0 - \varepsilon_\infty)$, α, and the mean relaxation time τ as fit parameters.

The temperature dependence of the inverse $\Delta\varepsilon$ and of the mean relaxation rate ($\nu = 1/2\pi\tau$) for peaks II and III for $x = 0.002$ are shown in the insets of Fig. 4 for the $x = 0.002$ sample. It is interesting to note that $\Delta\varepsilon$ of mode III increases with decreasing temperature and can be well described by a Curie-Weiss law with a Curie-Weiss temperature of

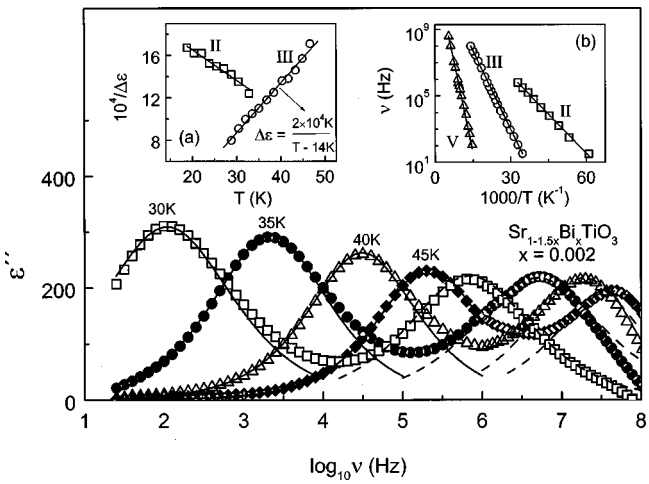

FIG. 4. Frequency dependence of ε'' for the dielectric peaks I and II for $(Sr_{1-1.5x}Bi_x)TiO_3$ with $x = 0.002$ for various temperatures. The solid and dashed lines are fitting curves to the Cole-Cole function Eq. (2) for modes III and II, respectively. Inset (a) shows the temperature dependence of $\Delta\varepsilon^{-1}$. The solid line for mode III is a fitting curve to the Curie-Weiss law. Inset (b) shows the temperature dependence of the relaxation rates. The solid lines are fitting curves to the Arrhenius law.

14 K [inset (a) in Fig. 4]. The mean relaxation rates for the modes II and III strictly follow an Arrhenius behavior, $\nu = \nu_0 \exp(-E/k_B T)$ [inset (b) in Fig. 4]. The energy barriers E and the attempt frequency ν_0 were found to be $E_{\mathrm{II}} = 400$ K, $\nu_{0,\mathrm{II}} = 1.6 \times 10^{11}$ Hz and $E_{\mathrm{III}} = 700$ K, $\nu_{0,\mathrm{III}} = 1.6 \times 10^{12}$ Hz for modes II and III, respectively.

The rate dependencies for the modes I and V were only determined from the maximum of the dielectric loss. Both of them also follow the Arrhenius relation. The inset (b) in Fig. 4 shows the Arrhenius behavior of the relaxation process V, with $E_{\mathrm{V}} = 1590\,\mathrm{K}$ and $\nu_{0,\mathrm{V}} = 1.6 \times 10^{12}\,\mathrm{Hz}$. For the relaxation mode I we found $E_{\mathrm{I}} = 133$ K and $\nu_{0,\mathrm{I}} = 0.8 \times 10^{10}$ Hz. The values for modes I and V are in good agreement with those found in nominally pure single-crystal STO.[8,19,20]

C. Analysis for $0 \leqslant x \leqslant 0.0267$

Also for the other concentrations investigated, the mean relaxation rates for modes II and III follow strictly an Arrhenius behavior in the experimentally accessible temperature window. The activation energies, the inverse attempt frequencies $\tau_0 (= 1/2\pi\nu_0)$, and the width parameter α for the modes II and III are shown in Fig. 5 as a function of the bismuth concentration x. Both τ_0 and E depend only slightly on concentration. ν_0 is of the order of a typical phonon frequency for all compounds. The activation energies increase on doping from 700 to 900 K for mode III and from 300 to 400 K for mode II. The width parameter α increases with increasing x, signaling an increasing width of the distribution of energy barriers on increasing doping.

Figure 6 shows the results for the concentration dependence of the inverse $\Delta\varepsilon$ for mode III in the upper panel and for mode II in the lower panel. For mode III, with increasing x, the inverse Curie-Weiss-like susceptibility for $x = 0.002$ becomes almost temperature independent for $x = 0.0067$, and finally reveals the behavior of an ordered polar system for

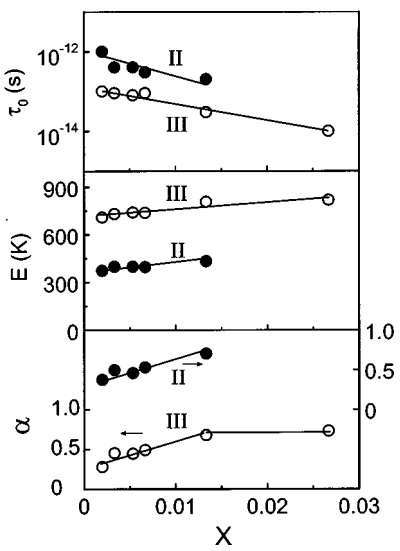

FIG. 5. Fitting parameters E, τ_0, and α as a function of Bi concentration x for peaks II and III in $(Sr_{1-1.5x}Bi_x)TiO_3$ samples. α for mode II was obtained at 22 K, and for mode III at 37 K. The lines are guides to the eyes.

$x=0.0133$ and 0.0267. For mode II, the inverse $\Delta\varepsilon$ always increases with decreasing temperature for all samples. These observations indicate a fundamentally different microscopic origin of mode II as compared with the behavior of mode III.

IV. DISCUSSION

In Ref. 15, some of the present authors attributed the dielectric anomaly in low Bi-doped STO ($x=0.002-0.0267$) to the occurrence of the quantum ferroelectric state mainly based on the consideration of the real part of the permittivity. In the present paper, we pay more attention to the imaginary part of the permittivity, which allows a more sensitive investigation of the relaxation processes. In addition we also extend the Bi concentration to a lower value, $x=0.0005$, and measure the permittivity down to 1.5 K. This provides more detailed information. The presence of the Barrett paraelectric background can be clearly seen due to the lower measurement temperatures available now. The results also show that the dielectric peaks superimpose on the Barrett paraelectric background for low Bi concentration ($0.0005\leqslant x\leqslant 0.0067$). Based on a close inspection of both ε' and ε'', we found that a number of dielectric modes exist in Bi-doped STO, and the peak position and activation energies of modes I, II, III, and V are essentially concentration independent in a wide concentration range. In fact, peak III is the one that was previously assumed as the quantum ferroelectric peak for $x=0.002$ in Ref. 15. The observed increase of the peak temperature T_m for ε' in Ref. 15 is due to the superposition effect of the unshifted mode III and the relaxor mode IV whose T_m clearly shifts to higher temperatures with increasing Bi concentration.[18] From this point of view, peak III can be denoted as a defect mode now.

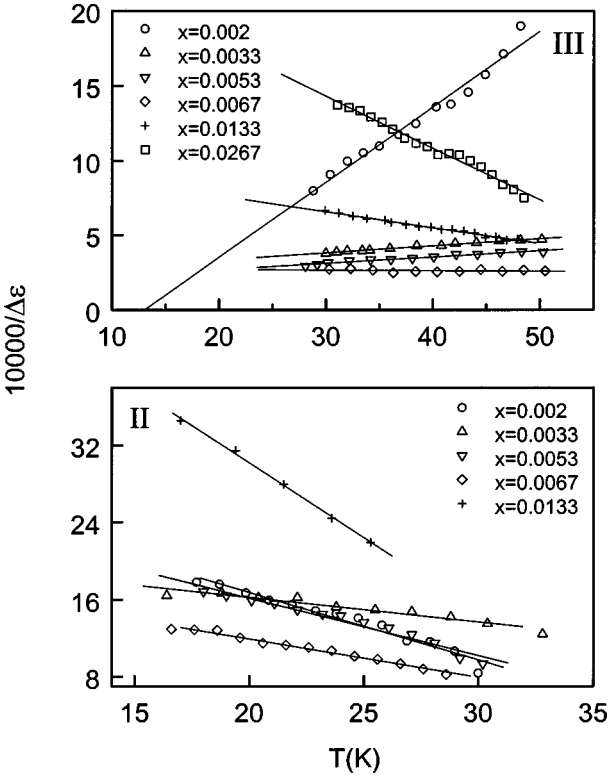

FIG. 6. Temperature dependence of the inverse susceptibilities for modes II (lower panel) and III (upper panel). The lines are linear fits.

In the present paper, we also observe that the paraelectric background of pure STO is almost monotonically reduced on doping with bismuth already at a ppm level of doping concentration. This provides strong experimental evidence for the formation of noninteracting polar clusters, which push the system off the quantum critical point. A straightforward explanation is that polar clusters are formed around the Bi defects, which are highly polarizable, possibly with the polarizability strongly enhanced via lattice deformations.[22] It seems reasonable that the dynamics of these noninteracting clusters shows up in the relaxation mode III. This mode shows Curie-Weiss behavior for the very low bismuth concentrations, but reveals decreasing $\Delta\varepsilon$ with decreasing temperature ($30<T<50$ K) for higher concentrations (upper panel of Fig. 6), while the paraelectric background still strongly increases. This behavior signals the appearance of local ordered regions within the long-range polar fluctuations of pure STO. Furthermore, the unshifted T_m implies that the clusters interact with some intrinsic mechanism of the host lattice. There may be a connection with the mode crossing point at around 37 K,[23] which gives an explanation of the unshifted T_m. In this picture it becomes plausible that the amplitude of mode III increases with x, as the coupling to the intrinsic mode becomes more effective with increasing x.

The energy barriers of mode III increase from 700 K ($x=0.002$) to approximately 900 K ($x=0.0267$). This concentration dependence of the energy barriers probably is due to lattice distortions and due to an increasing size of the clusters with increasing defect concentration. Concomitantly the increase in the width of the loss peak (see Fig. 5) signals an increasing distribution width of energy barriers.

As mentioned earlier, mode II behaves different compared to mode III. We suppose that mode II is of electronic origin. It is well known that in perovskite oxides, in many cases, especially, for the heterovalent substitution case, weakly bound electrons occur.[24,25] These weakly localized electrons could give rise to dielectric relaxation, which were found and

described in a variety of doped perovskites.[26,27] The relaxation processes were attributed to hopping of the polarons between lattice sites. In addition, the unshifted T_m of mode II also implies the possible interaction between the polarons and the intrinsic mechanism of the host lattice, such as phonon modes.

Mode I (8 K at 100 Hz) is also well established in nominally pure single-crystal STO.[20] It has been interpreted[20] in terms of a coherent quantum state.[28] However, we can detect these dielectric anomalies up to $x=0.0053$ in doped samples, in which quantum fluctuations are strongly suppressed and necessarily the system is far away from any coherent ground state. Hence we believe that this mode is a defect mode of unknown origin, even in the nominally pure STO. Recently Liu, Finlayson, and Smith, reported that the expansion of the tetragonal *c* axis with decreasing temperature below 105 K is arrested below 10 K,[29] and maybe mode I is related to the unknown defect interacting with this anomaly.

Mode V (65 K at 100 Hz) also appears in pure single-crystal STO,[19] and has been interpreted in terms of the ferroelastic domain-wall dynamics due to the cubic to tetragonal antidistortive phase transition close to 105 K in the undoped STO. We can detect this mode up to Bi concentrations $x \leqslant 0.0033$ before it merges into the broad relaxation of the relaxor phase (see Fig. 1). In the doped compounds this relaxation peak appears roughly at the same temperature, and its intensity changes with x, ranging between 40 and 62. Comparing with the small value of loss, ~ 1, in single-crystalline STO,[19] these values indicate that the amplitude of mode V is enhanced in polycrystals and by impurity doping. It seems reasonable that the density of domain walls in polycrystal or doped samples is higher than that in single crystals. Obviously, the domain-wall motion flips impurity dipoles or polar clusters which then contribute to the complex dielectric constant on the time scale of the domain dynamics.

V. CONCLUSIONS

We have presented a detailed report on the relaxation dynamics of bismuth-doped STO at low doping levels. On doping, the large paraelectric susceptibility of pure STO is strongly reduced. This fact signals the suppression of quantum fluctuations and concomitantly the appearance of polar clusters. We attribute mode III to the existence of noninteracting polar clusters, which seem to couple with some intrinsic mechanism of the host lattice. We explain mode II in terms of polaronic relaxation which is typically for doped perovskites. In addition we observed three further relaxation modes, two of which have also been observed on nominally pure single-crystal STO. Mode I which has been previously explained in terms of the coherent quantum state possibly is due to an impurity mode of unknown origin. Mode V seems to be induced by the ferroelastic domain-wall dynamics of the cubic to tetragonal phase transition. Mode IV will be discussed in the following paper.[18]

The present work shows that the dielectric response of Bi-doped STO is quite different from other doped quantum paraelectrics, for example, Ca-doped STO, or Li-doped KTO. A variety of relaxation modes was revealed in the present investigation and tentative explanations for their occurrence were proposed. Clearly, further work is necessary to arrive at a thorough understanding of the very rich relaxation behavior in this trivalent doped STO system.

*Permanent address: Department of Physics, Department of Materials Science and Engineering, Zhejiang University, Hangzhou, 310027, P.R. China.

[1] K. A. Müller and H. Burkhard, Phys. Rev. B **19**, 3593 (1979).
[2] M. E. Lines and A. M. Glass, *Principle and Application of Ferroelectrics and Related Materials* (Oxford University New York, 1977).
[3] G. I. Skanavi, I. M. Ksendzov, V. A. Trigubenko, and V. G. Prokhvatilov, Sov. Phys. JETP **6**, 250 (1958).
[4] J. G. Bednorz and K. A. Müller, Phys. Rev. Lett. **52**, 2289 (1984).
[5] U. T. Höchli, H. E. Weibel, and L. A. Boatner, Phys. Rev. Lett. **41**, 1410 (1978).
[6] G. A. Samara, Phys. Rev. Lett. **53**, 298 (1984).
[7] U. T. Höchli, K. Knorr, and A. Loidl, Adv. Phys. **39**, 405 (1990).
[8] J. Hemberger, M. Nicklas, R. Viana, P. Lunkenheimer, A. Loidl, and R. Böhmer, J. Phys.: Condens. Matter **8**, 4673 (1996).
[9] Y. Yacoby, Z. Phys. B **41**, 269 (1981).
[10] J. Toulouse, P. Diantonio, B. E. Vugmeister, X. M. Wang, and L. A. Knauss, Phys. Rev. Lett. **68**, 232 (1992).
[11] W. Kleemann, S. Kütz, and D. Rytz, Europhys. Lett. **4**, 239 (1987).
[12] T. Mitsui and W. B. Westphal, Phys. Rev. **124**, 1354 (1961).
[13] W. Kleemann, A. Albertini, R. V. Chamberlin, and J. G. Bednorz, Europhys. Lett. **37**, 145 (1997).
[14] R. V. Chamberlin, Phys. Rev. B **48**, 15 638 (1993); Europhys. Lett. **33**, 545 (1996).
[15] Chen Ang, Zhi Yu, P. M. Vilarinho, and J. L. Baptista, Phys. Rev. B **57**, 7403 (1998).
[16] Zhi Yu, Chen Ang, P. M. Vilarinho, and J. L. Baptista, J. Appl. Phys. **83**, 4874 (1998).
[17] Chen Ang, J. Scott, Zhi Yu, H. Ledbetter, and J. L. Baptista, preceding paper, Phys. Rev. B **59**, 6661 (1999).
[18] Chen Ang, Zhi Yu, P. Lunkenheimer, J. Hemberger, and A. Loidl, following paper, Phys. Rev. B **59**, 6670 (1999).
[19] R. Mizaras and A. Loidl, Phys. Rev. B **56**, 10 726 (1997).
[20] R. Viana, P. Lunkenheimer, J. Hemberger, R. Böhmer, and A. Loidl, Phys. Rev. B **50**, 601 (1994).
[21] J. H. Barrett, Phys. Rev. **86**, 118 (1952).
[22] M. G. Stacchiotti and R. Migoni, J. Phys.: Condens. Matter **2**, 4341 (1990).
[23] J. F. Scott, Ferroelectr. Lett. Sect. **20**, 89 (1995); J. F. Scott and H. Ledbetter, Z. Phys. B **104**, 635 (1997).
[24] R. Moos, A. Gnudi, and K. H. Hädtle, J. Appl. Phys. **78**, 5042 (1995).
[25] Yu Zhi, Ang Chen, P. M. Vilarinho, P. Q. Mantas, and J. L. Baptista, J. Eur. Ceram. Soc. **18**, 1613 (1998).
[26] E. Iguchi, N. Kubota, T. Nakamori, N. Yamamoto, and K. J. Lee, Phys. Rev. B **43**, 8646 (1991).
[27] O. Bidault, M. Maglione, M. Actis, M. Kchikech, and B. Salce, Phys. Rev. B **52**, 4191 (1995).
[28] K. A. Müller, W. Berlinger, and E. Tosatti, Z. Phys. B **84**, 277 (1991).
[29] M. Liu, T. R. Finlayson, and T. F. Smith, Phys. Rev. B **55**, 3480 (1997).